Search for a dark photon in the $\pi^0 \to e^+e^-\gamma$ decay

The WASA-at-COSY Collaboration

P. Adlarson[a], W. Augustyniak[b], W. Bardan[c], M. Bashkanov[d,e], F.S. Bergmann[f], M. Berłowski[g], H. Bhatt[h], A. Bondar[i], M. Büscher[j,k], H. Calén[a], I. Ciepał[c], H. Clement[d,e], D. Coderre[j,k,l], E. Czerwiński[c], K. Demmich[f], E. Doroshkevich[d,e], R. Engels[j,k], W. Erven[m,k], W. Eyrich[n], P. Fedorets[j,k,o], K. Föhl[p], K. Fransson[a], F. Goldenbaum[j,k], P. Goslawski[f], A. Goswami[q], K. Grigoryev[j,k,r], C.–O. Gullström[a], F. Hauenstein[n], L. Heijkenskjöld[a], V. Hejny[j,k], F. Hinterberger[s], M. Hodana[c,j,k], B. Höistad[a], A. Jany[c], B.R. Jany[c], L. Jarczyk[c], T. Johansson[a], B. Kamys[c], G. Kemmerling[m,k], F.A. Khan[j,k], A. Khoukaz[f], S. Kistryn[c], J. Klaja[c], H. Kleines[m,k], B. Kłos[t], M. Krapp[n], W. Krzemień[c], P. Kulessa[u], A. Kupść[a,g,*], A. Kuzmin[i], K. Lalwani[h,1], D. Lersch[j,k], L. Li[n], B. Lorentz[j,k], A. Magiera[c], R. Maier[j,k], P. Marciniewski[a], B. Mariański[b], U.–G. Meißner[j,k,v,s,w], M. Mikirtychiants[j,k,l,r], H.–P. Morsch[b], P. Moskal[c], B.K. Nandi[h], H. Ohm[j,k], I. Ozerianska[c], E. Perez del Rio[d,e], N. Piskunov[x], P. Pluciński[a,2], P. Podkopał[c,j,k], D. Prasuhn[j,k], A. Pricking[d,e], D. Pszczel[a,g], K. Pysz[u], A. Pyszniak[a,c], C.F. Redmer[a,3], J. Ritman[j,k,l], A. Roy[q], Z. Rudy[c], S. Sawant[h], S. Schadmand[j,k], A. Schmidt[n], T. Sefzick[j,k], V. Serdyuk[j,k,y], N. Shah[h,4], B. Shwartz[i], M. Siemaszko[t], R. Siudak[u], T. Skorodko[d,e], M. Skurzok[c], J. Smyrski[c], V. Sopov[o], R. Stassen[j,k], J. Stepaniak[g], E. Stephan[t], G. Sterzenbach[j,k], H. Stockhorst[j,k], H. Ströher[j,k], A. Szczurek[u], T. Tolba[j,k,5], A. Trzciński[b], R. Varma[h], G.J. Wagner[d,e], W. Węglorz[t], A. Wirzba[j,k,v], M. Wolke[a], A. Wrońska[c], P. Wüstner[m,k], P. Wurm[j,k], A. Yamamoto[z], J. Zabierowski[aa], M.J. Zieliński[c], W. Zipper[t], J. Złomańczuk[a], P. Żuprański[b], M. Żurek[c]

[a] *Division of Nuclear Physics, Department of Physics and Astronomy, Uppsala University, Box 516, 75120 Uppsala, Sweden*
[b] *Department of Nuclear Physics, National Centre for Nuclear Research, ul. Hoza 69, 00-681, Warsaw, Poland*
[c] *Institute of Physics, Jagiellonian University, ul. Reymonta 4, 30-059 Kraków, Poland*
[d] *Physikalisches Institut, Eberhard–Karls–Universität Tübingen, Auf der Morgenstelle 14, 72076 Tübingen, Germany*
[e] *Kepler Center for Astro and Particle Physics, Eberhard Karls University Tübingen, Auf der Morgenstelle 14, 72076 Tübingen, Germany*
[f] *Institut für Kernphysik, Westfälische Wilhelms–Universität Münster, Wilhelm–Klemm–Str. 9, 48149 Münster, Germany*
[g] *High Energy Physics Department, National Centre for Nuclear Research, ul. Hoza 69, 00-681, Warsaw, Poland*
[h] *Department of Physics, Indian Institute of Technology Bombay, Powai, Mumbai–400076, Maharashtra, India*
[i] *Budker Institute of Nuclear Physics of SB RAS, Academician Lavrentyev 11, Novosibirsk, 630090, Russia*
[j] *Institut für Kernphysik, Forschungszentrum Jülich, 52425 Jülich, Germany*
[k] *Jülich Center for Hadron Physics, Forschungszentrum Jülich, 52425 Jülich, Germany*
[l] *Institut für Experimentalphysik I, Ruhr–Universität Bochum, Universitätsstr. 150, 44780 Bochum, Germany*

[m] Zentralinstitut für Engineering, Elektronik und Analytik, Forschungszentrum Jülich, 52425 Jülich, Germany
[n] Physikalisches Institut, Friedrich–Alexander–Universität Erlangen–Nürnberg, Erwin–Rommel-Str. 1, 91058 Erlangen, Germany
[o] Institute for Theoretical and Experimental Physics, State Scientific Center of the Russian Federation, Bolshaya Cheremushkinskaya 25, 117218 Moscow, Russia
[p] II. Physikalisches Institut, Justus–Liebig–Universität Gießen, Heinrich–Buff–Ring 16, 35392 Giessen, Germany
[q] Department of Physics, Indian Institute of Technology Indore, Khandwa Road, Indore–452017, Madhya Pradesh, India
[r] High Energy Physics Division, Petersburg Nuclear Physics Institute, Orlova Rosha 2, Gatchina, Leningrad district 188300, Russia
[s] Helmholtz–Institut für Strahlen– und Kernphysik, Rheinische Friedrich–Wilhelms–Universität Bonn, Nußallee 14–16, 53115 Bonn, Germany
[t] August Chełkowski Institute of Physics, University of Silesia, Uniwersytecka 4, 40-007, Katowice, Poland
[u] The Henryk Niewodniczański Institute of Nuclear Physics, Polish Academy of Sciences, 152 Radzikowskiego St, 31-342 Kraków, Poland
[v] Institute for Advanced Simulation, Forschungszentrum Jülich, 52425 Jülich, Germany
[w] Bethe Center for Theoretical Physics, Rheinische Friedrich–Wilhelms–Universität Bonn, 53115 Bonn, Germany
[x] Veksler and Baldin Laboratory of High Energiy Physics, Joint Institute for Nuclear Physics, Joliot–Curie 6, 141980 Dubna, Moscow region, Russia
[y] Dzhelepov Laboratory of Nuclear Problems, Joint Institute for Nuclear Physics, Joliot–Curie 6, 141980 Dubna, Moscow region, Russia
[z] High Energy Accelerator Research Organisation KEK, Tsukuba, Ibaraki 305–0801, Japan
[aa] Department of Cosmic Ray Physics, National Centre for Nuclear Research, ul. Uniwersytecka 5, 90–950 Łódź, Poland

Abstract

The presently world largest data sample of $\pi^0 \to \gamma e^+ e^-$ decays containing nearly $5{\times}10^5$ events was collected using the WASA detector at COSY. A search for a dark photon U produced in the $\pi^0 \to \gamma U \to \gamma e^+ e^-$ decay from the $pp \to pp\pi^0$ reaction was carried out. An upper limit on the square of the $U - \gamma$ mixing strength parameter ϵ^2 of 5×10^{-6} at 90% CL was obtained for the mass range 30 MeV $< M_U <$ 90 MeV. This result together with other recent experimental limits significantly reduces the M_U *vs.* ϵ^2 parameter space preferred by the measured value of the muon anomalous magnetic moment.

Keywords: dark forces, gauge vector boson
PACS: 14.70.Pw, 13.20.Cz.

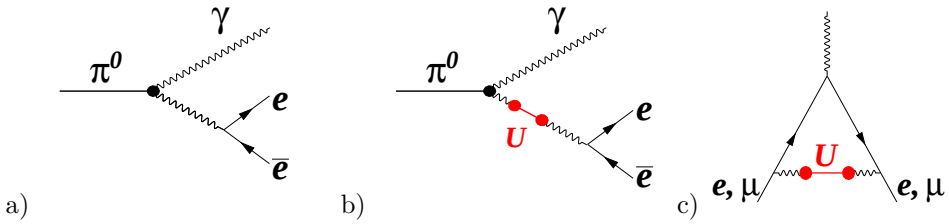

Figure 1: Feynman diagrams for a) the lowest order electromagnetic $\pi^0 \to e^+e^-\gamma$ decay and a possible contribution of U vector boson to: b) $\pi^0 \to e^+e^-\gamma$ and c) lepton $g-2$.

1. Introduction

Decays of neutral pseudoscalar mesons into a lepton-antilepton pair and a photon, $P \to l^+l^-\gamma$, are among the tools to search for a new light vector boson connected with dark gauge forces [1, 2, 3]. The boson is postulated in several theoretical models to be responsible for the annihilation of dark matter particles. Such annihilation into an e^+e^- pair could explain the positron and/or electron excesses observed by PAMELA [4], ATIC [5] and H.E.S.S. [6] as well as the narrow 0.511 MeV γ ray emission from the galactic bulge observed by INTEGRAL [7].

In one of the simplest scenarios dark matter particles belonging to an additional abelian gauge symmetry are added to the Standard Model (SM). The new symmetry leaves the SM particles unchanged [8, 9, 3, 10]. The associated gauge boson can communicate with the SM through a small mixing in the kinetic term of the QED Lagrangian [11]:

$$\mathcal{L}_{\rm mix} = -\frac{\epsilon}{2} F^{\rm QED}_{\mu\nu} F^{\mu\nu}_{\rm dark} \tag{1}$$

where ϵ is the mixing parameter. The gauge boson U (or A') is often called a *dark photon* since it can mix with the photon in all processes (examples are shown in Figs. 1b) and c). General theoretical arguments [12, 13] suggest that the ϵ parameter must be of the order of $10^{-4} - 10^{-2}$ and the boson mass M_U

*Corresponding author
Email address: andrzej.kupsc@physics.uu.se (A. Kupść)
[1]present address: Department of Physics and Astrophysics, University of Delhi, Delhi–110007, India
[2]present address: Department of Physics, Stockholm University, Roslagstullsbacken 21, AlbaNova, 10691 Stockholm, Sweden
[3]present address: Institut für Kernphysik, Johannes Gutenberg–Universität Mainz, Johann–Joachim–Becher Weg 45, 55128 Mainz, Germany
[4]present address: Department of Physics and Astronomy, University of California, Los Angeles, California–90045, U.S.A.
[5]present address: Albert Einstein Center for Fundamental Physics, Fachbereich Physik und Astronomie, Universität Bern, Sidlerstr. 5, 3012 Bern, Switzerland

below 1 GeV. This estimate is also supported by the astrophysical observations and the constraints imposed by precision measurements such as the anomalous magnetic moments $(g-2)$ of muon and electron [14]. The contribution of the U boson to the $(g-2)_l$ $(l = e, \mu)$ is given in [14] by:

$$\Delta(g-2)_l = \frac{\alpha\epsilon^2}{2\pi}\int_0^1 dz \frac{2m_l^2 z(1-z)^2}{m_l^2(1-z)^2 + M_U^2 z} = \begin{cases} \frac{\alpha\epsilon^2}{2\pi}, & \text{if } M_U \ll m_l \\ \frac{\alpha\epsilon^2}{2\pi}\frac{2}{3}\left(\frac{m_l}{M_U}\right)^2, & \text{if } M_U \gg m_l \end{cases} . \tag{2}$$

Investigations of the M_U *vs.* ϵ^2 parameter space corresponding to the experimentally preferred $(g-2)_\mu$ value (shifted by $+3 \times 10^{-9}$ with respect to the SM value [15]) are therefore of great importance.

The U boson is expected to be a narrow resonance. For a U boson with mass less than twice the muon mass the total decay width is for all practical purposes (neglecting higher-order electric, tiny weak interaction contributions from the U boson – Z_0 coupling, and the decay to light dark scalars and/or fermions) given by [16, 17]:

$$\Gamma_U = \Gamma_{U\to e^+e^-} = \frac{1}{3}\alpha\epsilon^2 M_U \sqrt{1-\frac{4m_e^2}{M_U^2}}\left(1+\frac{2m_e^2}{M_U^2}\right), \tag{3}$$

where m_e is the electron mass.

Such a light U boson can be directly produced in particle accelerators, see *e.g.* Refs [16, 17, 18, 19, 20, 21, 22, 23, 24]. The idea is to search for narrow structures in the invariant mass spectrum of the lepton-antilepton pair.

The M_U *vs.* ϵ^2 region corresponding to the measured $(g-2)_\mu$ value $\pm 2\sigma$ is covered by the data from the BABAR [25], MAMI A1 [26], KLOE-2 [27] and APEX [28] experiments for M_U masses above 100 MeV. On the lower end this preferred region is excluded by the $(g-2)_e$ value for $M_U < 30$ MeV [29, 30]. In addition, ϵ regions below 10^{-6} are excluded by experiments which are sensitive to lepton pairs from displaced secondary vertices ($\tau_U > 10^{-11}$ s) [31, 32, 33].

Our experiment aims at searching for a short-lived U boson in the π^0 Dalitz decay, $\pi^0 \to e^+e^-\gamma$, covering the range preferred by the experimental value of $(g-2)_\mu$ for 30 MeV$< M_U <$ 100 MeV. In this region, for $\epsilon > 10^{-3}$ the average distance passed by a boson emitted from a low energy π^0 decay should be less than a millimeter. The best limit from a previous $\pi^0 \to e^+e^-\gamma$ experiment with the origin of the e^+e^- pair close to the production vertex was obtained by the SINDRUM collaboration more than twenty years ago [34, 35]. The SINDRUM result is based on a sample of 98400 $\pi^0 \to e^+e^-\gamma$ decays with e^+e^- invariant masses above 25 MeV.

2. The Experiment

The WASA detector setup was built and first used at CELSIUS in Uppsala and moved to COSY (COoler SYnchrotron) Jülich in the Summer of 2005 [36]. The detector was designed and optimized for studies of rare π^0 meson decays

produced in hadronic interactions [37]. It consists of three main components: The Forward Detector (FD) – covering scattering angles in the $3^\circ - 18^\circ$ range used for tagging and triggering of meson production, the Central Detector (CD) – used for measuring meson decay products, and the pellet target system. The target beam consists of 20 – 30 μm diameter pellets of hydrogen, providing an areal target density in the order of 10^{15} atoms/cm^2. The diameter of the pellet beam is ~ 3.8 mm.

The CD surrounds the interaction region and is designed to detect and identify photons, electrons, and charged pions. It consists of an inner drift chamber (MDC), a superconducting solenoid providing the magnetic field for momentum determination, a barrel of thin plastic scintillators (PS) for particle identification and triggering, and an electromagnetic calorimeter. The amount of structural material is kept to a minimum to reduce the amount of secondary interactions outside of the detector sensitive volumes. The beryllium beam pipe (diameter 6 cm) wall is 1.2 mm thick and the material of the superconducting solenoid corresponds to 0.18 radiation lengths.

The FD allows identification and reconstruction of protons from the $pp \to pp\pi^0$ reaction close to threshold. The track coordinates are provided by four sets of straw proportional chambers. Kinetic energies are reconstructed using the ΔE information in layers of plastic scintillators of different thickness. In addition, the signals are used for triggering. The kinetic energy, T, of the protons can be reconstructed with a resolution of $\sigma(T)/T \sim 1.5 - 3\%$ for kinetic energies below 400 MeV.

The results presented here are based on data collected during one-week WASA-at-COSY run carried out in 2010. The π^0 mesons were produced in proton–proton interactions at a kinetic beam energy of 550 MeV. The beam energy corresponds to the center-of-mass excess energy of 122 MeV with respect to $pp\pi^0$ threshold (*i.e.* below two pion production thresholds) with a cross section of 1.12 mb [38]. The maximum scattering angle of the outgoing protons for the reaction is 45°. For detection and for triggering purposes the phase space of the $pp \to pp\pi^0$ reaction can be divided into three regions:

1. Both protons are measured in the FD. This corresponds to a geometrical acceptance of 19%.
2. One proton is measured in the FD and one in the forward part of the PS (scattering angles $20^\circ - 40^\circ$). This corresponds to a geometrical acceptance of 42%.
3. Both protons are registered in the PS. This corresponds to a geometrical acceptance of 21%.

Case (1) allows the definition of the most selective trigger condition and the best resolution in the missing mass with respect to the two protons. Therefore, the main trigger for the experiment required two tracks in the FD. The protons from the $pp \to pp\pi^0$ reaction have a maximum kinetic energy of 350 MeV and are mostly stopped in the FD. This allows the inclusion of a veto from a thin plastic detector layer placed at the far end of the FD into the trigger condition. In addition, two hits in the central part of the PS (scattering angles $45^\circ - 135^\circ$)

were required, aiming to select the electron-positron pair. An additional, scaled down, trigger based on case (2) was used in parallel. The WASA-at-COSY data acquisition system allowed the collection of more than 10^4 events per second and the luminosity was set to optimize the conditions for the main trigger. The integrated luminosity of the run was about 0.55 pb^{-1}.

The data quality is illustrated by analysis of the main trigger data sample and requesting in the analysis two identified (using $\Delta E/\Delta E$ method) FD proton tracks. An electron positron pair is selected by requiring two oppositely curved tracks in the MDC with scattering angles between 40° and 140°. A photon hit cluster in the calorimeter with an energy deposit above 20 MeV is also requested. The missing mass squared with respect to two protons ($MM^2(pp)$) for the above selection is shown in Fig. 2a. In addition to the $pp \to pp\pi^0$ reaction signal one sees also a contribution due to random coincidences of $pp \to pp$ and $pp \to pn\pi^+$ reactions. This background is effectively suppressed by including electron and positron identification using the reconstructed momentum and the energy deposit in the calorimeter. The corresponding $MM(pp)$ plot after this cut is shown in Fig. 2b. The $\pi^0 \to e^+e^-\gamma$ decay is independently identified from the invariant mass of the decay products $IM(e^+e^-\gamma)$ (calculated assuming the tracks originate at the beam target crossing) shown in Fig. 2c. The data are well described by a simulation of $pp \to pp\pi^0$ with $\pi^0 \to e^+e^-\gamma$ and $\pi^0 \to \gamma\gamma$ decays, where in the latter case one of the two photons converts in the beryllium beam tube.

For Monte Carlo simulations, angular distributions for the $pp \to pp\pi^0$ reaction from [38] were used in the event generation. The $\pi^0 \to e^+e^-\gamma$ decay is generated using the lowest order QED matrix element squared:

$$|\mathcal{A}|^2 = \Gamma_{\gamma\gamma} 16\pi^3 M \frac{\alpha}{\pi}\frac{1}{q^2}\left(1-\frac{q^2}{M^2}\right)^2\left(1+\cos^2\theta^* + \frac{4m_e^2}{q^2}\sin^2\theta^*\right)|F(q^2)|^2 \quad (4)$$

where θ^* is the angle of e^+ in the dilepton rest frame with respect to the dilepton momentum in the overall π^0 decay system, M and m_e are π^0 and $e^\pm$ masses respectively, $\Gamma_{\gamma\gamma}$ is the partial $\pi^0 \to \gamma\gamma$ decay width, and $F(q^2)$ (with q^2 the squared momentum transfer of the off-shell photon) is the π^0 transition form factor. The form factor close to $q^2 = 0$ is parametrized as: $F(q^2) = 1 + aq^2/M^2$. The value of the dimensionless linear coefficient a is 0.032 ± 0.004 [39]. Consequently, for the range of q considered in this work the form factor can be safely approximated by one.

The matrix element from Eqn. (4) leads to the following unperturbed $d\Gamma/dq$ distribution [40] for the standard lowest order electromagnetic decay $\pi^0 \to e^+e^-\gamma$ of Fig. 1a:

$$\frac{d\Gamma}{dq} = \Gamma_{\gamma\gamma}\frac{4\alpha}{3\pi}\frac{1}{q}\sqrt{1-\frac{4m_e^2}{q^2}}\left(1+\frac{2m_e^2}{q^2}\right)\left(1-\frac{q^2}{M^2}\right)^3|F(q^2)|^2. \quad (5)$$

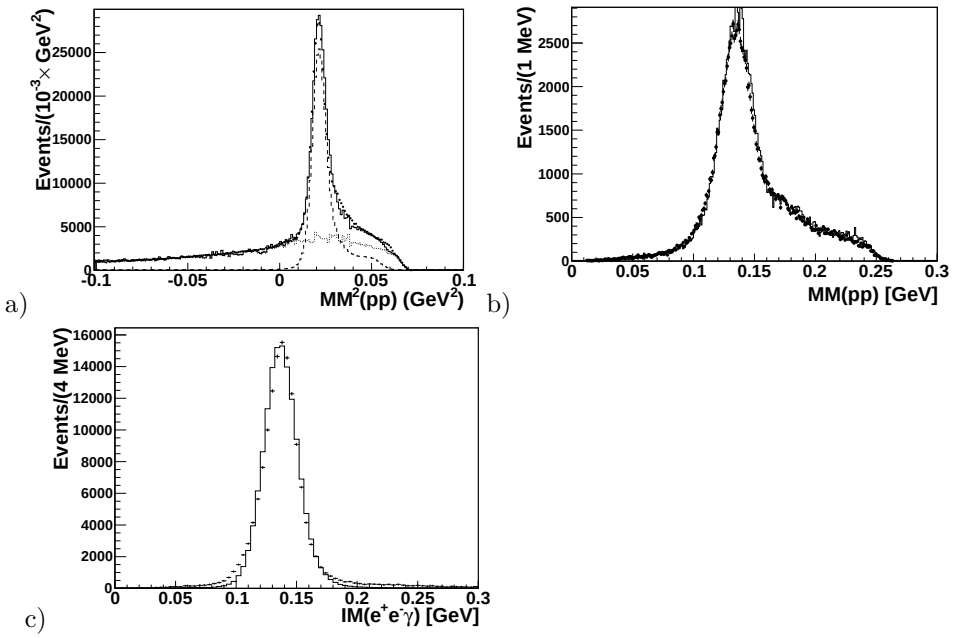

Figure 2: Control data sample with two protons, an e^+e^- pair and a photon. a) Distribution of the missing mass squared with respect to the two protons registered in the FD before electron identification. Experimental data (black points); simulations: $\pi^0 \to e^+e^-\gamma$ and $\pi^0 \to \gamma\gamma$ (broken line), random coincidences of two events (dotted line), and the sum (solid line). b) Distribution of $MM(pp)$ after electron identification: experimental data (black points) and sum of Monte Carlo simulations (solid line). c) The reconstructed invariant mass of the $e^+e^-\gamma$ system after particle identification cut.

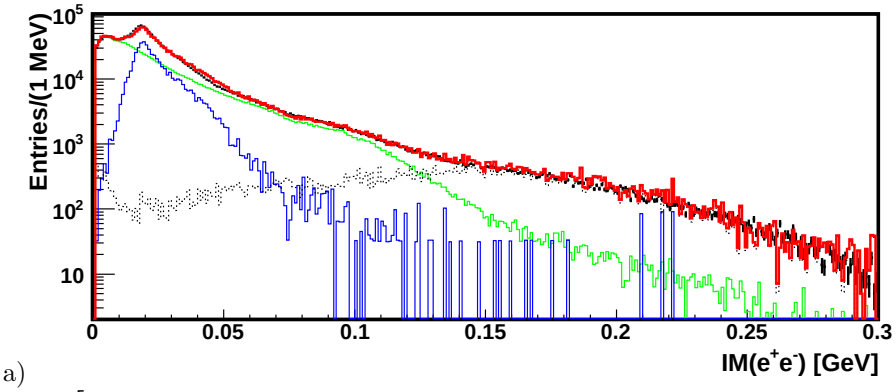

a)

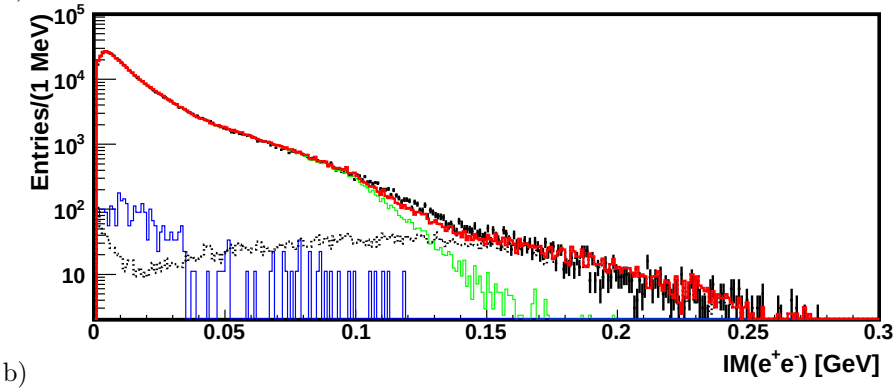

b)

Figure 3: The reconstructed e^+e^- invariant mass $q = IM(e^+e^-)$: a) before and b) after the cuts for reducing the conversion background. The experimental data are denoted by black points. Results of simulations for $\pi^0 \to \gamma\gamma$ (blue line) and $\pi^0 \to e^+e^-\gamma$ (green line) decays are normalized according to the known branching ratios. The normalization of random coincidences (dotted line) was fitted in order to reproduce the $IM(e^+e^-) > 150$ MeV range. The sum of all simulated contributions is given by the red line.

3. Data analysis

The first stage of data analysis is to extract a clean signal of $\pi^0 \to e^+e^-\gamma$ decays. The results shown in the previous section suggest that at this energy electron-positron pairs come nearly exclusively from the π^0 meson decays. Therefore, in order to maximize the yield of the $\pi^0 \to \gamma e^+e^-$ events we use an inclusive data sample requesting events with (i) at least one proton identified in the FD, (ii) an e^+e^- pair identified in the CD. There is no request of an additional photon cluster and we have included events from both triggers corresponding to phase space regions (1) and (2). The distribution of the reconstructed invariant mass of the electron-positron pair, $q = IM(e^+e^-)$, is shown in Fig. 3a. This spectrum is well described by the sum of $\pi^0 \to e^+e^-\gamma$ and $\pi^0 \to \gamma\gamma$ (with photon conversion). The data sample contains $1.8{\times}10^6$ reconstructed events.

The $\pi^0 \to \gamma\gamma$ events are efficiently removed by a condition on the recon-

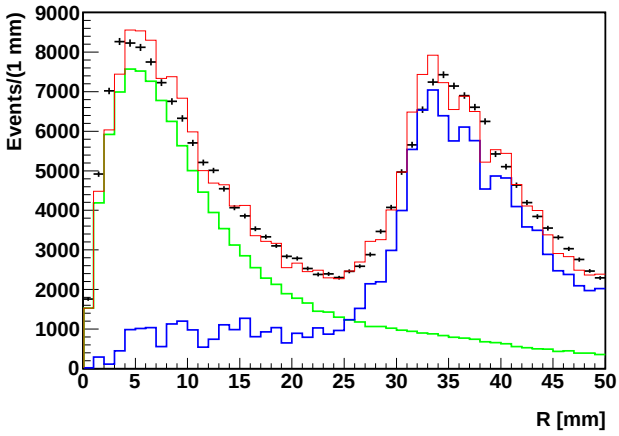

Figure 4: Distribution of the distance R between the COSY beam axis and the reconstructed point of closest approach of e^+ and e^- tracks: experimental data (black crosses); simulations for $\pi^0 \to \gamma\gamma$ (blue line), the $\pi^0 \to e^+e^-\gamma$ decay (green line), and the sum of the two contributions (red line).

structed position of the e^+e^- vertex. Fig. 4 shows the distance (R) of the reconstructed vertex from the COSY beam axis. The contributions of the $\pi^0 \to \gamma\gamma$ and $\pi^0 \to e^+e^-\gamma$ decays, simulated according to the known branching ratios, are in very good agreement with the observed distribution and they are well separated. In order to further reduce the external conversion background one uses the invariant mass of the e^+e^- calculated from the momentum directions at the points where the tracks intersect the beam tube, IM_b, shown in Fig. 5. The selection cut is performed in the IM_b *vs.* R plane (Fig. 5). The cut removes 98% of the $\pi^0 \to \gamma\gamma$ events which contribute to $IM(e^+e^-)$ distribution due to conversion.

The finally reconstructed dN/dq distribution, containing nearly $5{\times}10^5$ entries, is shown in Fig. 3b. It is well described by the simulations of the $\pi^0 \to e^+e^-\gamma$ decay channel alone with a very small (approx. 3000 events) admixture of background from the $\pi^0 \to \gamma\gamma$ decay. The data in this work represent the world largest data sample of $\pi^0 \to e^+e^-\gamma$ events, which is almost an order of magnitude larger than the sample used for the previously published results from the SINDRUM experiment [34, 41].

3.1. Upper limit for the $BR(\pi^0 \to \gamma(U \to e^+e^-))$

A distinctive feature of the expected signal of the decay $\pi^0 \to \gamma(U \to e^+e^-)$ (Fig. 1b) is the appearance of a narrow peak (the width being given by the detector resolution) in the invariant mass distribution of the electron positron pair at the U boson mass. The electrodynamics process $\pi^0 \to \gamma^*\gamma \to e^+e^-\gamma$ (Fig. 1a) both represents the irreducible background and is used for normalization. Due to the expected small decay width of the U boson the interference

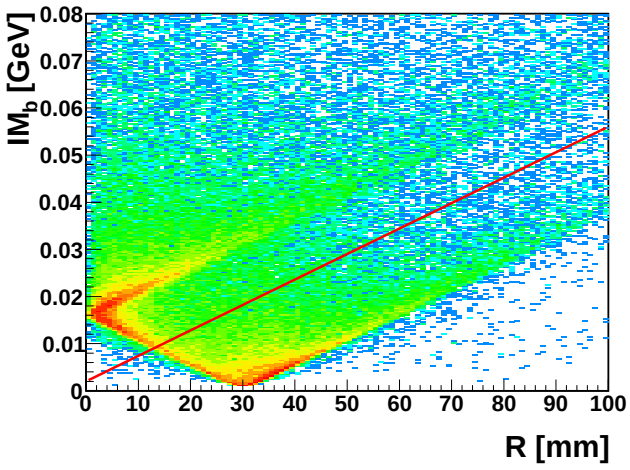

Figure 5: Correlation between R and IM_b variables for the experimental data. The selection cut is shown by the diagonal line. The events below the line mainly come from photon conversions in the beam pipe.

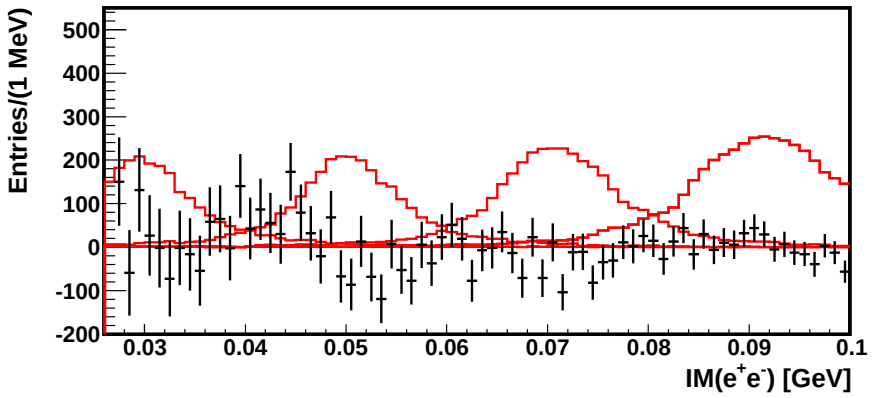

Figure 6: Difference between the reconstructed e^+e^- invariant mass distribution and the sum of all simulated contributions (black points). The resolution and sensitivity are illustrated by the superimposed red histograms. They represent the signals expected for the $\pi^0 \to U\gamma \to e^+e^-\gamma$ process with U boson masses of $M_U = 30$, 50, 70 and 90 MeV and $BR(\pi^0 \to U\gamma) = 10^{-4}$ (the corresponding ϵ values are: 0.0077, 0.0088, 0.0113, and 0.0169 respectively).

term is negligible and the signal from the U boson can be tested by constructing an incoherent sum of the two contributions.

The experimental data are described well by the simulation based on Eqn. (4) alone as shown in Fig. 3. The difference between reconstructed experimental q distribution and the sum of all simulated contributions is given in Fig. 6. In addition there are superimposed five example distributions corresponding to the $\pi^0 \to U\gamma \to e^+e^-\gamma$ process for U boson masses of 30, 50, 70 and 90 MeV respectively, assuming $BR(\pi^0 \to U\gamma) = 10^{-4}$. The plots illustrate both the resolution and the efficiency expected for the signal.

For a given value of U boson mass corresponding to the range of k^{th} bin of the invariant mass spectrum ($q_k < M_U < q_k + \Delta q$, with $\Delta q = 1$ MeV the width of the histogram bin) the number of events in the i^{th} bin of the reconstructed electron-positron invariant mass distribution, N_i, can be described in the following form:

$$N_i/N_{Tot} = \frac{1}{\Gamma}\sum_j S_{ij}\eta_j\nu_j + S_{ik}\eta_k\beta \tag{6}$$

The first term in the Eqn. (6) represents the contribution from the Dalitz decay and the second term from the hypothetical $\pi^0 \to \gamma(U \to e^+e^-)$ decay chain. Indices j and k label the *true, unperturbed* distributions and i the reconstructed q histogram. N_{Tot} is total number of produced π^0 mesons, $1/\Gamma$ is the π^0 life time and η_j is the efficiency. S_{ij} is the normalized smearing matrix (for each j: $\sum_i S_{ij} = 1$), ν_j is the unperturbed $d\Gamma/dq$ distribution for the $\pi^0 \to e^+e^-\gamma$ decay (Eqn. (5)) integrated over bin j:

$$\nu_j \equiv \int_{q_j}^{q_j+\Delta q} \frac{d\Gamma}{dq} dq, \tag{7}$$

and β is $BR(\pi^0 \to \gamma(U \to e^+e^-))$. The efficiency and the smearing matrix was obtained from the detector simulation. The U boson decay mechanism in diagram Fig. 1b implies that the efficiencies as a function of $\cos\theta^*$ are identical to the ones of the $\pi^0 \to e^+e^-\gamma$ decay with $q = M_U$. Note that for the quoted values of the branching ratios the intrinsic width (3) of the U boson would be in the eV range and thus very much smaller than the experimental bin size.

The upper limits for the U boson branching ratios, β, as a function of M_U were obtained by repeating for all bins (index k in Eqn. (6)), corresponding to the 30 MeV $< M_U <$ 100 MeV range, the least square fits of Eqn. (6) to the experimental q distribution. Fig. 7 shows the 90% CL upper limits obtained for the branching ratio of $\pi^0 \to \gamma(U \to e^+e^-)$ decay as a function of the assumed value of M_U. This result is compared to that obtained from the SINDRUM data [34].

The branching ratio of $\pi^0 \to \gamma U$ is related to ϵ^2 by [42, 18]:

$$\frac{\Gamma(\pi^0 \to \gamma U)}{\Gamma(\pi^0 \to \gamma\gamma)} = 2\epsilon^2 |F(M_U^2)|^2 \left(1 - \frac{M_U^2}{M^2}\right)^3. \tag{8}$$

The resulting upper limits for the ϵ^2 parameter is shown in Fig. 8 and compared with other experiments.

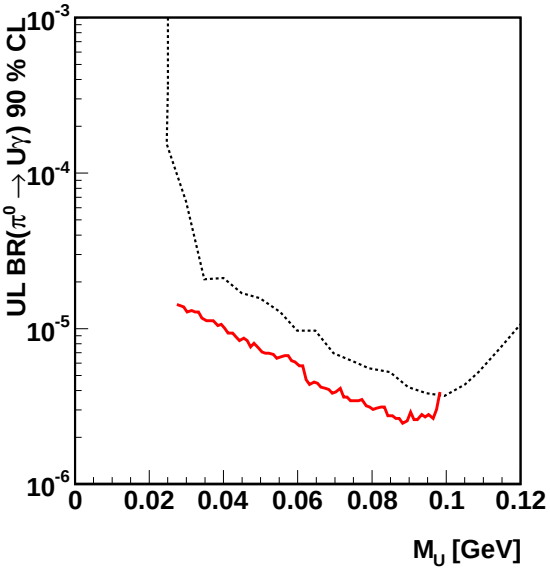

Figure 7: A 90% C.L. upper limit for the $BR(\pi^0 \to \gamma U)$ from this paper (solid line) compared to the result of the SINDRUM experiment [34] (dotted line).

The recent limits for the electron $g-2$ are taken from Refs [30, 29]. Our upper limit is compatible with the combined KLOE limits [43] using a disparate experimental setup and different meson decay as source of e^+e^- pairs. Together they significantly reduce the parameter space for mass and mixing strength of a hypothetical dark photon U, if the latter is assumed to account for the present experimental value of the muon anomalous magnetic moment. The experiment presented in the paper if repeated with an order of magnitude larger statistics would cover the remaining part of this region of interest. The collected data can also be used for to determine the π^0 transition form factor.

Acknowledgments

This work was supported in part by the EU Integrated Infrastructure Initiative HadronPhysics Project under contract number RII3-CT-2004-506078; by the European Commission under the 7th Framework Programme through the 'Research Infrastructures' action of the 'Capacities' Programme, Call: FP7-INFRASTRUCTURES-2008-1, Grant Agreement N. 227431; by the Polish National Science Centre through the Grants No. 86/2/N-DFG/07/2011/0 0320/B/H03/2011/40, 2011/01/B/ST2/00431, 2011/03/B/ST2/01847, 0312/B/H03/2011/40. We gratefully acknowledge the support given by the Swedish Research Council, the Knut and Alice Wallenberg Foundation, and the Forschungszentrum Jülich FFE Funding Program of the Jülich Center for Hadron Physics.

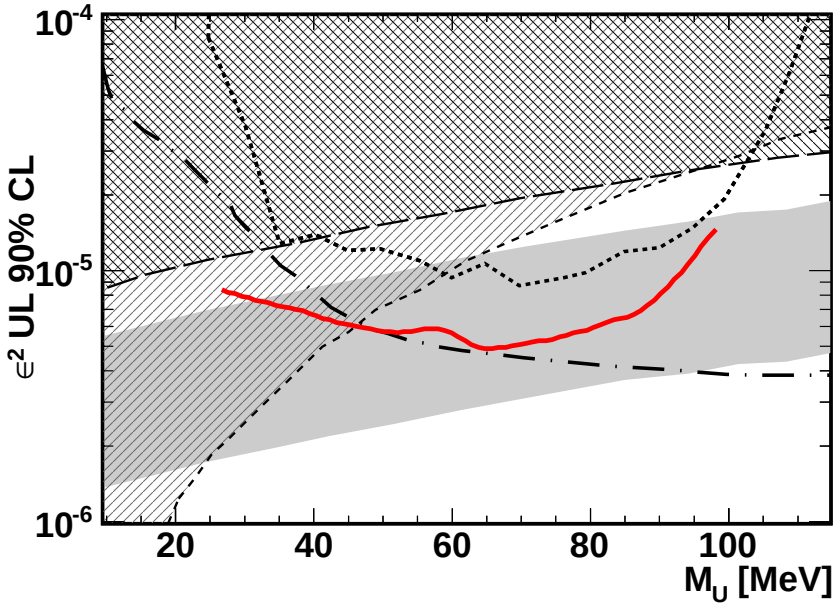

Figure 8: Summary of the 90% CL upper limits for the mixing parameter ϵ^2 from WASA-at-COSY (red solid line) compared to SINDRUM $\pi^0 \to e^+e^-\gamma$ [34] (dotted line) and recent combined KLOE $\phi \to \eta e^+e^-$ [43] (dashed dotted) upper limits. The long respectively short dashed lines (and the corresponding hatched areas) are the upper limits derived from the muon and the electron $g-2$ [29]. In addition the gray area represents the $\pm 2\sigma$ preferred band around the present value of the muon $g-2$.

The authors thank technical staff at Forschungszentrum Jülich for support in preparation of and during the experiment.

This work is part of the PhD Thesis of C.-O. Gullström.

References

[1] P. Fayet, Phys.Lett. B95 (1980) 285.

[2] M. Dobroliubov and A.Y. Ignatiev, Phys.Lett. B206 (1988) 346.

[3] C. Boehm and P. Fayet, Nucl.Phys. B683 (2004) 219, arXiv:hep-ph/0305261.

[4] PAMELA Collaboration, O. Adriani et al., Nature 458 (2009) 607, arXiv:0810.4995.

[5] J. Chang et al., Nature 456 (2008) 362.

[6] H.E.S.S. Collaboration, F. Aharonian et al., Phys.Rev.Lett. 101 (2008) 261104, arXiv:0811.3894.

[7] P. Jean et al., Astron.Astrophys. 407 (2003) L55, arXiv:astro-ph/0309484.

[8] P. Fayet, Nucl.Phys. B187 (1981) 184.

[9] B. Holdom, Phys.Lett. B166 (1986) 196.

[10] M. Pospelov, A. Ritz and M.B. Voloshin, Phys.Lett. B662 (2008) 53, arXiv:0711.4866.

[11] L. Okun, Sov.Phys.JETP 56 (1982) 502.

[12] N. Arkani-Hamed et al., Phys.Rev. D79 (2009) 015014, arXiv:0810.0713.

[13] K.R. Dienes, C.F. Kolda and J. March-Russell, Nucl.Phys. B492 (1997) 104, arXiv:hep-ph/9610479.

[14] M. Pospelov, Phys.Rev. D80 (2009) 095002, arXiv:0811.1030.

[15] Muon G-2 Collaboration, G. Bennett et al., Phys.Rev. D73 (2006) 072003, arXiv:hep-ex/0602035.

[16] J.D. Bjorken et al., Phys.Rev. D80 (2009) 075018, arXiv:0906.0580.

[17] B. Batell, M. Pospelov and A. Ritz, Phys.Rev. D79 (2009) 115008, arXiv:0903.0363.

[18] M. Reece and L.T. Wang, JHEP 0907 (2009) 051, arXiv:0904.1743.

[19] M. Freytsis, G. Ovanesyan and J. Thaler, JHEP 1001 (2010) 111, arXiv:0909.2862.

[20] N. Borodatchenkova, D. Choudhury and M. Drees, Phys.Rev.Lett. 96 (2006) 141802, arXiv:hep-ph/0510147.

[21] P.f. Yin, J. Liu and S.h. Zhu, Phys.Lett. B679 (2009) 362, arXiv:0904.4644.

[22] R. Essig, P. Schuster and N. Toro, Phys.Rev. D80 (2009) 015003, arXiv:0903.3941.

[23] M. Baumgart et al., JHEP 0904 (2009) 014, arXiv:0901.0283.

[24] H.B. Li and T. Luo, Phys.Lett. B686 (2010) 249, arXiv:0911.2067.

[25] BABAR Collaboration, B. Aubert et al., Phys.Rev.Lett. 103 (2009) 081803, arXiv:0905.4539.

[26] A1 Collaboration, H. Merkel et al., Phys.Rev.Lett. 106 (2011) 251802, arXiv:1101.4091.

[27] F. Archilli et al., Phys.Lett. B706 (2012) 251, arXiv:1110.0411.

[28] APEX Collaboration, S. Abrahamyan et al., Phys.Rev.Lett. 107 (2011) 191804, arXiv:1108.2750.

[29] M. Endo, K. Hamaguchi and G. Mishima, Phys.Rev. D86 (2012) 095029, arXiv:1209.2558.

[30] T. Aoyama et al., Phys.Rev.Lett. 109 (2012) 111807, arXiv:1205.5368.

[31] Crystal Barrel Collaboration, C. Amsler et al., Phys.Lett. B333 (1994) 271.

[32] NOMAD Collaboration, J. Altegoer et al., Phys.Lett. B428 (1998) 197, arXiv:hep-ex/9804003.

[33] S. Gninenko, Phys.Rev. D85 (2012) 055027, arXiv:1112.5438.

[34] SINDRUM I Collaboration, R. Meijer Drees et al., Phys.Rev.Lett. 68 (1992) 3845.

[35] S. Gninenko, (2013), arXiv:1301.7555.

[36] WASA-at-COSY Collaboration, H.H. Adam et al., (2004), arXiv:nucl-ex/0411038.

[37] CELSIUS/WASA Collaboration, C. Bargholtz et al., Nucl.Instrum.Meth. A594 (2008) 339, arXiv:0803.2657.

[38] G. Rappenecker et al., Nucl.Phys. A590 (1995) 763.

[39] Particle Data Group, J. Beringer et al., Phys.Rev. D86 (2012) 010001.

[40] L. Landsberg, Phys.Rept. 128 (1985) 301.

[41] SINDRUM I Collaboration, R. Meijer Drees et al., Phys.Rev. D45 (1992) 1439.

[42] B. Batell, M. Pospelov and A. Ritz, Phys.Rev. D80 (2009) 095024, arXiv:0906.5614.

[43] KLOE-2 Collaboration, D. Babusci et al., Phys.Lett. B720 (2013) 111, arXiv:1210.3927.